

Review

Comprehensive mitral valve prolapse assessment by cardiovascular MRI



F. Musella^{a,*,1}, A. Azzu^{b,c,1}, A.S. Antonopoulos^d, L. La Mura^a,
R.H. Mohiaddin^{b,c,**}

^a Department of Advanced Biomedical Sciences, University Federico II of Naples, Naples, Italy

^b Royal Brompton and Harefield Hospitals, Guy's and St Thomas' NHS Foundation Trust, UK

^c National Heart and Lung Institute, Imperial College London, UK

^d 1st Cardiology Department, Athens School of Medicine, National and Kapodistrian University of Athens, Athens, Greece

ARTICLE INFORMATION

Article history:

Received 17 July 2021

Accepted 5 November 2021

Mitral valve (MV) prolapse (MVP) is a not fully understood common MV disorder. The development of sophisticated cardiovascular magnetic resonance imaging (CMRI) sequences over the last decades has allowed a more detailed assessment and provided better understanding of the pathophysiology of MVP to guide management, interventions, and risk stratification of patients affected. This review provides an overview of the most recent insights about this multifaceted pathology, particularly regarding the emerging concepts of mitral annular disjunction (MAD), and risk of arrhythmia and sudden death associated with myocardial fibrosis. We describe the emerging role of CMRI in both diagnosis and, more importantly, risk assessment of this disease, aiming to provide a comprehensive protocol for the assessment of MVP, which could represent a practical guide to clinicians and MRI practitioners working in the field.

© 2021 The Royal College of Radiologists. Published by Elsevier Ltd. All rights reserved.

Introduction

Mitral valve (MV) prolapse (MVP) is a common disorder, characterised by superior displacement of the leaflets into the left atrium (LA). MVP is a clinical entity that is not fully understood, despite being known for more than a century.¹ The development of sophisticated cardiovascular magnetic resonance imaging (CMRI) sequences over the last decades has

allowed more detailed assessment of MVP and provided insight and better understanding of its pathophysiology. CMRI affords the advantage of assessing the severity of mitral regurgitation (MR) associated with MVP, LA size, biventricular volumes/function, and to exclude concurrent and coexisting cardiovascular abnormalities of connective tissue disorders, such as Marfan syndrome.² Most importantly, recent studies have shown the value of native myocardial T1 mapping and

* Guarantor and correspondent: F. Musella, Department of Advanced Biomedical Sciences, University Federico II of Naples, Naples, Italy. Tel.: +393336544924.

** Guarantor and correspondent: R.H. Mohiaddin, Royal Brompton and Harefield Hospitals, Guy's and St Thomas' NHS Foundation Trust, National Heart and Lung Institute, Imperial College London.

E-mail addresses: francmusella@gmail.com (F. Musella), R.Mohiaddin@rbht.nhs.uk (R.H. Mohiaddin).

¹ These authors contributed equally to the study.

late gadolinium enhancement (LGE) for the assessment of myocardial fibrosis and risk prognostication. As such, there is a growing need for the establishment of a standardised CMRI protocol for comprehensive and detailed study of MVP.

Normal MV anatomy and nomenclature

MV apparatus comprises mitral leaflets, mitral annulus, chordae tendineae, and papillary muscles (PMs). The two mitral leaflets are described as posterior and anterior. The posterior leaflet is commonly divided into three scallops by the presence of indentations, or clefts, which partially extend from the free edge into the body of the leaflet (known as P1, P2, and P3). Although the free edge of the anterior leaflet is free from indentations, three virtual scallops A1–3 corresponding to the described posterior scallops are also identified (Fig 1).

The MV leaflets are attached to the PMs by sets of tendinous chordae that are classified in three orders according to their site of insertion to the leaflets. The primary chordae are multiple and thin and insert on the free edge of the leaflet; the secondary chordae attach on the ventricular surface of the body of the leaflet, among them two are stronger and thicker (strut chordae); the tertiary chordae origin from the ventricular wall and insert to the basal portion of the posterior leaflet only. Tendinous chordae arise from the tips of two main PMs known as anterolateral and posteromedial according to their position in the mid-apical LV wall.

Clinical classification and phenotypes of MVP

MVP is usually classified as primary (or non-syndromic) and secondary (or syndromic) when encountered in the setting of certain syndromes (Table 1).³ Non-syndromic MVP is an inherited condition with variable penetrance and high phenotypic variability within the same family. Common genetic syndromes that cause MVP include aortopathies such as Marfan and Loey–Dietz syndromes. Other syndromes, such as trisomies 18, 13, and 15, lead to cardiac malformations and valvulopathies including MVP. Patients with collagenopathies such as Ehlers–Danlos syndrome may also present with MVP. Other classical causes of MVP include syndromes that affect skeletal muscles including pseudoxanthoma elasticum, osteogenesis imperfecta, Larsen-like syndrome, Borrone dermato-

Table 1

Clinical classification (syndromic versus non-syndromic MVP).

Syndromic MVP	
Marfan syndrome/MASS phenotypes	
Loeys–Dietz	
Aneurysm–osteoarthritis syndrome	
Ehlers–Danlos syndrome	
Juvenile polyposis syndrome	
Osteogenesis imperfecta	
Pseudoxanthoma elasticum	
BDCS or FTH syndromes	
Larsen-like syndrome	
Williams–Beuren syndrome	
Syndrome with sinus node dysfunction, arrhythmias, LVNC (HCN4)	
Trisomies 18, 13, 15	
Non-syndromic MVP	
MMVP1 (16p11.2–p12.1 locus)	
MMVP2 (11p15.4 locus)	
MMVP3 (13q31.3–31.2 locus)	
Filamin A-MVP (FLNA)	
DCHS1	
Dilated cardiomyopathy (FLNC, LMNA)	

MASS, mitral valve prolapse (M), nonprogressive aortic root dilatation (A), musculoskeletal findings (S), and skin striae (S); BDCS, Borrone dermatocardio-skeletal; FTH, Frank-Ter Haar; LVNC, left ventricular non-compaction; HCN4, hyperpolarisation-activated cyclic nucleotide channel 4; MMVP, myxomatous mitral valve prolapse; FLNA, Filamin-A; DCHS1, Dachous1; FLNC, Filamin-C; LMNA, Lamin-A.

cardio-skeletal and Frank–Ter Haar syndromes.⁴ MVP can also present in the context of genetic dilated cardiomyopathies.

Further to its clinical classification, the MVP phenotype exhibits high variability (Table 2). On one side of the spectrum is the typical Barlow’s disease phenotype, affecting the spongiosa, characterised by myxomatous degeneration of the mitral leaflets, which are thickened, elongated, and prolapse. On the other side of the spectrum is the clinical phenotype of fibroelastic deficiency (FED) with the typical features of thin, translucent leaflets of normal length in older patients, associated with chordal rupture. In FED, histology demonstrates deficiency in collagen, elastin, and proteoglycans. It should be noted that these two clinical phenotypes (FED and Barlow’s disease) are the two opposite ends of the spectrum, and that in everyday clinical practice or within members of the same family, there are overlapping phenotypes.

Diagnosis of MVP

The diagnosis of MVP relies predominantly on trans-thoracic echocardiography (TTE). Based on the M-mode

Table 2

Phenotypes (Barlow versus fibroelastic) of mitral valve prolapse.

Characteristics	Fibroelastic	Barlow
Age at diagnosis	>60 years	<60 years
History of MR	<5 years	>5 years
Leaflet tissue	Normal	+++
Anterior leaflet tissue	+	+++
Posterior leaflet tissue	++	+++
Segment affected	Single segment (P2)	Multisegment
Chordae tendinae	Thin and ruptured	Thickened and elongated
Annular dilatation	≤32mm	≥36 mm
Calcification	None	+++

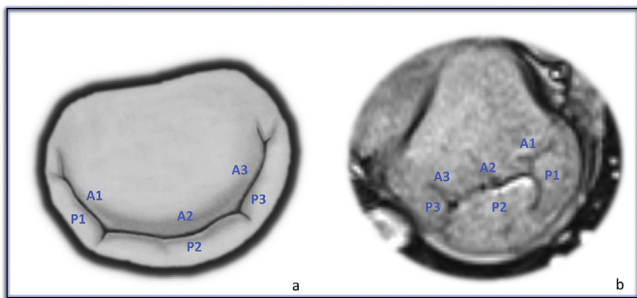


Figure 1 (a) Surgical view of the mitral valve scallops as seen from the left atrium. (b) CMRI “en face” view of the mitral valve scallops as seen from the left ventricle (b).

findings, the definition of MVP includes posterior displacement of one or both leaflets ≥ 2 mm during late systole or holosystolic displacement > 3 mm.⁵ On two-dimensional (2D) echocardiography, MVP diagnosis is based on parasternal long axis (PLAX) findings, where a uni- or bi-leaflet systolic displacement during coaptation towards the atrial side of the annulus, with no strict consensus 2D criteria for the degree of displacement. Other echocardiographic findings may include the myxomatous appearance with thickening and elongation of the leaflets, various degrees of MR ranging from absent to severe forms, LA dilatation, with mitral annulus disjunction (MAD) and hyper-tractility of the basal inferolateral wall. Transoesophageal echocardiography (TOE) allows a better visualisation of MV anatomy in MVP and assessment of the exact mechanisms of MR, the number of prolapsing scallops, etc. It also provides a detailed en-face view of the MV,

like that seen by the surgeon from a LA perspective (the so-called “surgical view”), thus facilitating operative planning.

Over the last decades, CMRI has gained growing influence in the evaluation of MVP, providing additional information to the conventional echocardiographic assessment (Table 3). On CMRI, there are no strict criteria for the diagnosis of MVP, although the typical M-mode definition of 2 mm seems to have excellent diagnostic accuracy for MVP when using echocardiography as the reference standard.⁵ MVP diagnosis on CMRI typically relies on recognition of other typical features, such as inspection of MV leaflet for billowing, leaflet thickening/elongation, mitral annular dilatation, and visualisation of the mitral regurgitation jet. Other features may include a mildly dilated and hypokinetic LV with typically hypercontractile basal inferolateral wall.⁶ On LGE sequences, there might be LV wall and PMS enhancement as well as hyper-enhancement of the fibrotic leaflets.

Prognosis of MVP

Overall, MVP is a benign condition with favourable prognosis and estimated mortality risk of 5% at 10 years.⁷ Although most patients with MVP remain asymptomatic and without complications throughout their lifespan, approximately 10% of MVP patients present with progressive deterioration to severe MR, as well as heart failure and pulmonary hypertension. In a community cohort of 833 MVP patients, moderate to severe MR and left ventricular ejection fraction (LVEF) $< 50\%$ were the strongest independent predictors of cardiovascular mortality. Other secondary risk factors for cardiovascular morbidity were mild MR, LA diameter ≥ 40 mm, flail leaflet, atrial fibrillation, and an age ≥ 50 years.⁷

In addition, certain subgroups of patients with MVP may be at increased risk for arrhythmias and sudden cardiac death (SCD) even in the absence of significant mitral regurgitation (MR). A recent study from Essayagh *et al.*⁸ in a cohort of 595 consecutive patients with MVP, demonstrated that ventricular arrhythmias are frequent but rarely severe. The incidence of ventricular arrhythmias was independently and strongly associated with specific electrocardiography (ECG) and morphological patterns particularly ST-T changes, the presence of MAD, and marked leaflet redundancy, which suggested a higher risk phenotype, independent of MR severity. Long-term severe arrhythmia was associated with long-term excess mortality and lower event-free survival.⁸

Triggered arrhythmias may result either from a pathological substrate, i.e. LV or PMS scarring as the result of increased transmitted tension from chordae to sub-valvular apparatus, or even by the redundant tissue valve prolapsing into the atrium in systole and ventricle in diastole.

Overall, the established markers of arrhythmic/SCD risk in patients with MVP used in clinical practice are: severe MR, LV systolic dysfunction, documented ventricular arrhythmias, T-wave inversion in inferior leads, LV fibrosis in inferolateral wall by CMRI, and family history of SCD.⁹

Table 3

Echocardiography versus cardiac magnetic resonance imaging in mitral valve prolapse assessment.

	PROS	CONS
ECHO	<ul style="list-style-type: none"> • Portability and availability • High temporal resolution • Visualisation of mitral valve scallops and subvalvular apparatus • Assessment of valvular calcifications • Assessment of left atrial size • Assessment of bi-ventricular size and function • Qualitative and quantitative assessment of mitral regurgitation • Quantification of pulmonary pressures • Identification and quantification of mitral annular disjunction • Visualisation of aortic root and thoracic aorta • Identification of associated abnormalities (e.g., atrial septal defect, Ebstein's) • Intraoperative assessment with transoesophageal study 	<ul style="list-style-type: none"> • Limited cut planes • Operator dependent • Acoustic window limitations • Depending on geometric assumptions • Caveats in assessment of eccentric jets • Semi-invasive if trans-oesophageal study
CMRI	<ul style="list-style-type: none"> • No body habitus/acoustic window limitations • Multiple imaging planes • Accurate and reproducible • Visualisation of mitral valve scallops on multiple planes • Assessment of subvalvular apparatus • Assessment of left atrial size • Ventricular measurements without geometrical assumptions • Qualitative assessment of mitral regurgitation • Accurate quantitative assessment of mitral regurgitation (also for eccentric jets) • Identification and quantification of mitral annular disjunction • Visualisation of aorta in toto • Identification of associated abnormalities (e.g., atrial septal defect, Ebstein's) • Detection of myocardial fibrosis 	<ul style="list-style-type: none"> • Not widely available • Claustrophobia • Difficulties in breath-holding • Longer time of acquisition • Compromised quality in case of arrhythmias • Lower temporal resolution

Mitral annular disjunction and myocardial fibrosis: emerging concepts and clinical implications

MAD was first described more than three decades ago as an abnormal atrial displacement of the hinge point of the MV away from the ventricular myocardium, closely linked to MVP.^{10–14} Carmo *et al.*¹¹ described MAD as a localised abnormality usually affecting the ventricular myocardium directly under the posterior mitral valve leaflet, typically in the region of the P1 and P2 mitral valve scallops. Imaging can detect not only the presence of MAD but also its location and extent as well as the degree of associated myxomatous MV disease and MR.¹⁵

MAD is detectable during ventricular systole only when the mitral annulus “slides” and detaches from the ventricular myocardium by a variable distance ranging from a few millimetres to >10 mm.¹² On echocardiography, this is most commonly seen in the PLAX view. This “abnormal movement” seems to contribute to annulus distortion and systolic dysfunction as well as to accelerated progression of the underlying MV disease, leading to more complex MV lesions.^{11,12,14} It has been hypothesised that MAD may be a precursor of degenerative MV disease and MVP, and according to recent data, it is independently associated with greater LV dimensions.¹⁶

According to several reports, palpitations are the most commonly reported symptom in patients with MAD, along with frequent premature ventricular contractions. The disjunctive areas along the mitral annulus may represent vulnerable areas to longstanding mechanical stress and clinical series have demonstrated that MAD is potentially responsible for sustained ventricular tachycardia (VT) and SCD, independently of concomitant MVP.^{8,11,16,17} In a cohort of 595 patients with isolated MVP, MAD was independently associated with long-term excess incidence of clinical arrhythmic events but not with excess mortality within 10 years from diagnosis.¹⁶ Markers of ventricular arrhythmias are younger age, previous syncope, premature ventricular contractions, PMs fibrosis, and MAD distance.¹⁷ An increased risk of arrhythmia has been associated with MAD distance >8.5 mm.^{11,15} CMRI may enhance risk stratification by detecting myocardial fibrosis (most frequently involving the basal inferior/inferolateral segments and the PMs) and measuring MAD distance in the inferolateral wall.^{15,18,19} Mantegazza *et al.*²⁰ supported these findings and proposed that patients without MAD on TTE but typical MAD-related symptoms or arrhythmias on ECG/Holter should be additionally evaluated by TOE or CMRI.

To conclude, MAD is a rare morphological abnormality seen in some patients with MVP, which can lead to an increased risk of malignant ventricular arrhythmias and SCD. Thus, there is a need to use multiple diagnostic tools to help identify patients with MAD at increased risk of malignant arrhythmias that may benefit from additional interventions (e.g., ICD implantation, VT ablation, or MV surgery).

Proposed CMRI protocol for the comprehensive assessment of MVP

Assessment of MVP requires detailed study not only of valve morphology to identify the involved scallops, but also thorough analysis of mitral sub-valvular apparatus, identification of MAD, and myocardial fibrosis. CMRI provides an excellent visualisation and understanding of MR mechanism and quantification of regurgitant volume/fraction along with a comprehensive assessment of LA dimensions and biventricular function and size.

In the following paragraph, we provide a detailed description of suggested steps that should be followed when scanning MVP to obtain all the above information and identify possible associated anomalies (Fig 2).

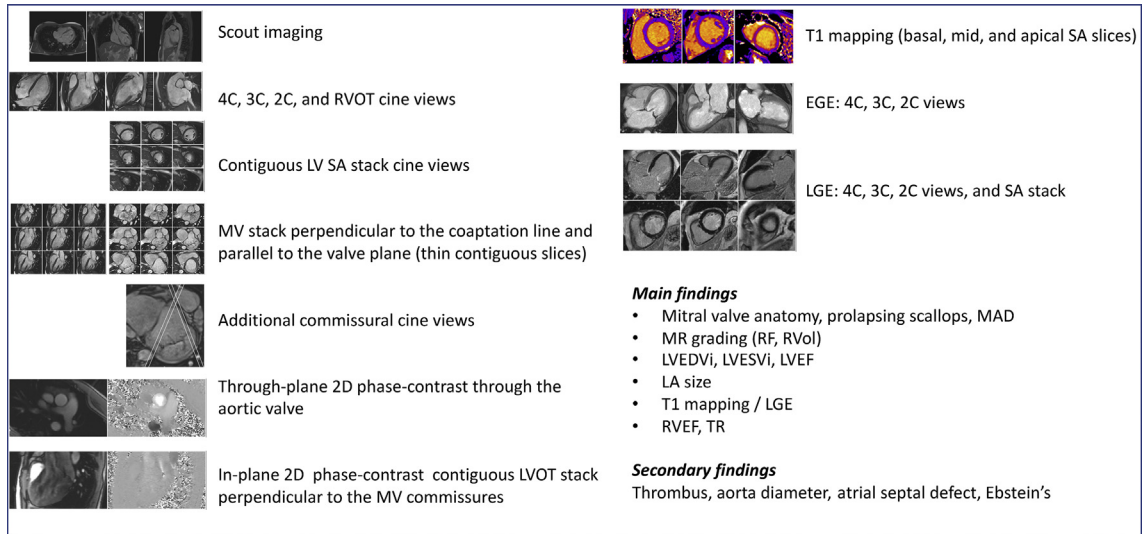
MV scallop assessment and sub-valvular apparatus visualisation

A thorough assessment of the MV anatomy and function is required to detect the mechanism underlying MR. Steady state free precession (SSFP) cine images acquired in standard two-chamber (2C), three-chamber (3C), four-chamber (4C) views, and short axis (SA) stack (from the mitral annulus to the LV apex) allow visualisation of the MV apparatus; however, a thorough imaging of the MV scallops requires acquisition of additional imaging planes. A stack of slices perpendicular to the central part of the coaptation line (from the en-face valve view) and parallel to the three-chamber view allows a comprehensive assessment of the mitral valve scallops from A1-P1, adjacent to the anterolateral commissure, to A3-P3, close to the posteromedial commissure, passing through A2-P2 in the middle (Fig 3a and b). By using a section thickness of 5 mm with no intersection gap, 2–3 sections per scallop are usually obtained. Additional cine images may be needed for an accurate visualisation of the commissural regions as the two ends of the coaptation line often have oblique orientation. A stack of thin slices parallel to the valvular plane may further improve the ability to identify the mechanism of mitral regurgitation and detect the origin of the regurgitation jet (Fig 3c and d).

PMs anatomy and function are usually assessed on long-axis and mid-ventricular SA cine images (Electronic [Supplementary Material Fig. S1](#)); however, if PMs pathology is suspected, an accurate evaluation requires 3D-SSFP sequences, which allow multiplanar reconstructions.

Evaluation of MAD

ECG-gated, breath-hold, SSFP images need to be acquired in the 2C, 3C, and 4C long-axis views, and a SA stack covering the entire LV (6-mm sections without a gap, 10–15 sections). The length of MAD is measured from the LA wall–posterior MV leaflet junction to the top of the LV inferior and lateral walls during end systole from 2C, 3C (Electronic [Supplementary Material Fig. S2a,b](#)), and 4C LV long-axis views.²¹ Mantegazza *et al.*²⁰ consider as reference any MV annulus detachment ≥ 2 mm detected by CMRI. As a



4C: 4-chamber; 3C: 3-chamber; 2C: 2-chamber; RVOT: right ventricular outflow tract; LV: left ventricular; SA: short-axis; MV: mitral valve; LVOT: left ventricular outflow tract; EGE: early gadolinium enhancement, LGE: late gadolinium enhancement; MR: mitral regurgitation; RF: regurgitant fraction; RVol: regurgitant volume; MAD: mitral annular disjunction; LVEDVi: left ventricular end-diastolic volume index; LVESVi: left ventricular end-systolic volume index; LVEF: left ventricular ejection fraction; LA: left atrium; RVEF: right ventricular ejection fraction, TR: tricuspid regurgitation.

Figure 2 Comprehensive protocol for the assessment of mitral valve prolapse. Sequences suggested for a proper morphological and functional assessment of MV and ventricles, quantification of MR, identification of MAD, fibrosis, and associated findings.

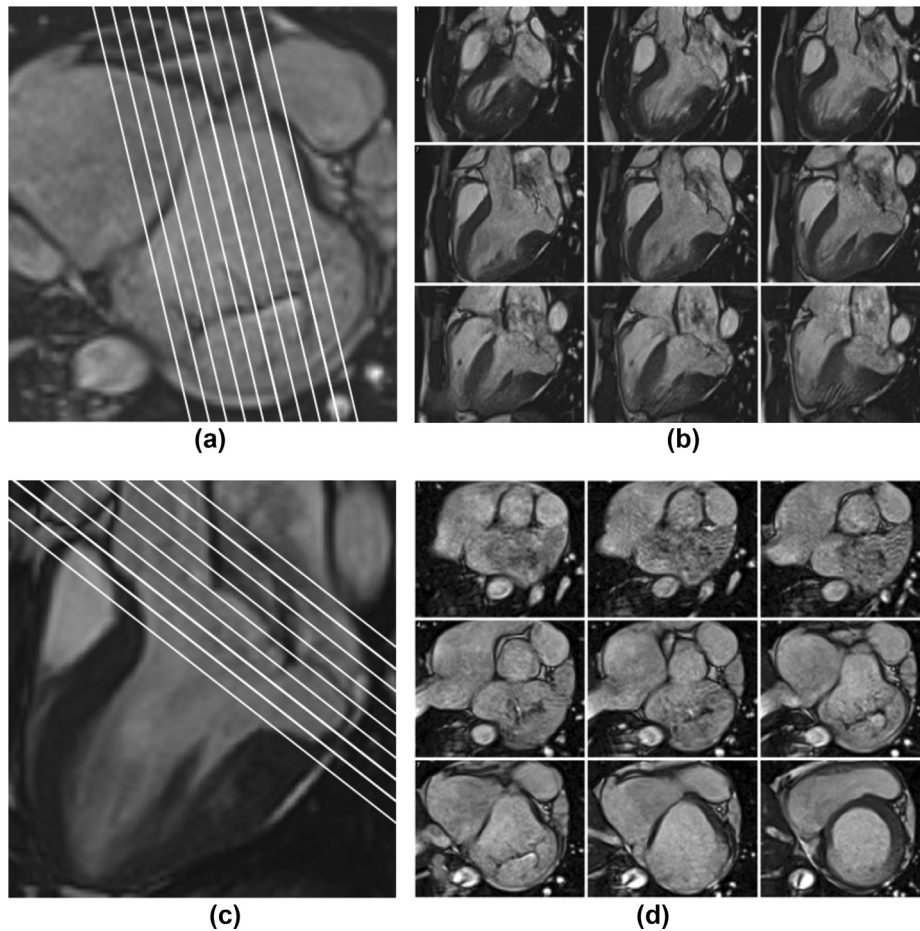


Figure 3 Planning for mitral valve detailed scanning. Planning an “en-face view” (a) to obtain a mitral valve long-axis stack (b). Planning on 3C view (c) to obtain a mitral valve short-axis stack (d).

routine evaluation of MAD, it would be important to span the entire MV annulus circumference as the MAD can extend differently along the valve ring.^{14,17} Although several studies have suggested that the greater the extent of MAD, the higher the arrhythmic risk is, there is no consensus on whether a specific cut-off in MAD length is associated with malignant ventricular arrhythmias.^{10,11,17,22} The motion of the mitral annulus is passive and determined by the contraction and relaxation of adjacent atrial and ventricular musculature. In normal conditions, the posterior mitral ring and its adjacent myocardium move downwards and anteriorly in systole, in synchrony with the remainder of the LV. In MAD patients, due to annular hypermobility, the severity of unusual systolic motion of the posterior mitral ring on the adjacent myocardium of the posterior MV leaflet (defined as *systolic curling*) is associated with the length of MAD. The quantitative assessment of curling is provided by tracing a line between the displaced LV inferior/inferolateral wall and the LA wall–posterior MV leaflet junction, and from this line, a perpendicular line to the lower limit of the mitral annulus in end systole (a detailed description is provided in Electronic [Supplementary Material Fig. S2c](#)).¹⁰

More recently, Zia *et al.*²³ demonstrated the existence of focal LV hypertrophy in the basal inferior/inferolateral wall in MVP patients. A positive correlation between the degree of basal LV hypertrophy and the excursion of the MV annulus has been found. The abnormal contractility of this LV region accounts in part for the so-called systolic curling motion.²³ Therefore, the presence or absence of focal LV hypertrophy should be included in the global assessment of MAD.

Assessment of mitral regurgitation

Echocardiography remains the most established imaging method for the initial assessment and follow-up of patients with MR; however, it can be often limited by poor acoustic window related to body habitus. Furthermore, MR can arise from primary abnormalities of any part of the MV apparatus (organic) or be secondary to geometrical remodelling of the LV (functional). Consequently, the regurgitant jets may vary in their anatomical and haemodynamic features and may not be fully investigated by echocardiography. Notably, a poor agreement between CMRI and TTE-derived MR grading in patients with late systolic and multiple jets in the context of organic MR has been reported.²⁴ This highlights how CMRI-derived regurgitant volume (RVol) can better identify patients with severe MR, who warrant close follow-up and, perhaps, earlier referral for MV surgery.²⁴

Qualitative assessment

The CMRI SSFP sequence offers high intrinsic contrast between blood and the surrounding cardiac structures, thus allowing investigation of the blood flow pattern (manifest as areas of MR signal void). Disease severity can be visually graded according to the extent of signal loss into the proximal chamber (LA, Electronic [Supplementary Material Fig. S3](#)), ranging from grade 1 in cases with signal loss

limited to the valve plane, to grade 4 showing signal loss throughout half of systole. This is a semi-quantitative method, with unsatisfactory reproducibility as it is operator dependent and the extent of signal loss can be influenced by acquisition parameters, such as echo time (TE). Nevertheless, visualisation of distal flow disturbance remains useful for the detection of regurgitation and evaluation of MR jet origin and direction. Through-plane velocity mapping is also recommended for a qualitative assessment (rather than quantitative) of the regurgitation jet(s) on the atrial side of the coaptation. In conclusion, a CMRI study should always seek to identify the origin, direction, and extension of the regurgitant jet, as these are key elements in both the diagnosis and management of the MV disease.

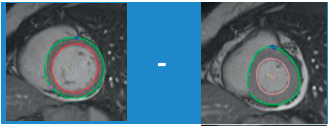
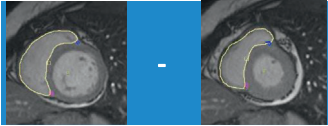
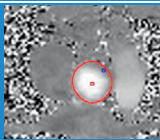
Quantitative assessment

The key parameters for the quantitative grading of MR are regurgitant volume (RVol) and regurgitation fraction (RF). RVol represents the amount of blood flowing retrogradely in the LA during each systole, while RF is derived from the ratio between RVol and the total stroke volume (SV) expressed as a percentage.²⁵ When dealing with semilunar valves, phase contrast sequences can directly quantify the anterograde and retrograde flow volume. On the contrary, phase contrast imaging of MV is challenging because of the movement of the mitral annulus during systole requiring alternative indirect approaches.²⁵ In normal haemodynamic conditions, the LVSV (calculated as difference between end-diastolic and end-systolic volume) equals the RVSV, and these match the blood volume measured on through-plane phase-contrast sequences across aortic (Qs) and pulmonary (Qp) valves respectively ([Table 4](#)). Given the above, in the absence of other regurgitant lesions, MV-RVol can be calculated by subtracting the RVSV from the LVSV; however, the calculation of RVSV is less reproducible compared to LVSV due to the extensive trabeculation of RV.²⁶ Moreover, associated tricuspid regurgitation is reported in a high percentage of patients with significant MR, and this invalidates the use of RVSV to determine the RVol. A more accurate method to quantify the amount of blood flowing retrogradely in the atrium rather than crossing the aortic plane during the LV contraction, namely the RVol, is to subtract the aortic flow from LVSV. This method of quantifying mitral regurgitation applies even in the presence of aortic regurgitation as long as only the systolic forward flow in the aorta is taken as the aortic SV.²⁶

CMRI reference values for MR quantification, although not as firmly established as in echocardiography, have been recently reported in a consensus statement by Garg *et al.*²⁷ and are outlined in [Table 5](#).

Although the 2D phase-contrast sequences are considered the standard approach to MR quantification, 4D phase-contrast flow imaging is increasingly used to study the haemodynamic of valves and shunts. This technique allows tracking of valve motion throughout the cardiac cycle and direct measurement of MR, this being particularly useful in pathologies involving multiple valves.²⁸ Fidock *et al.*²⁹

Table 4
Quantitative assessment of mitral regurgitation.

LVSV =	LVEDV - LVESV	
RVSV =	RVEDV - RVESV	
Mitral Rvol =	LVSV - RVSV	
Mitral Rvol = LVSV = Qs in the absence of MR	LVSV - Qs	LVSV - 
RF % =	100 x RVol / LVSV	

LVSV: left ventricular stroke volume; LVEDV: left ventricular end-diastolic volume; LVESV: left ventricular end-systolic volume; RVSV: right ventricular stroke volume; RVEDV: right ventricular end-diastolic volume; RVSEV: right ventricular end-systolic volume; RVol: regurgitant volume; Qs: systemic flow; RF: regurgitant fraction.

recently demonstrated that 4D flow-derived MR volume is similar to that derived using 3D TOE, and shows high reproducibility and consistency. As such, 4D phase-contrast flow imaging could be considered in those centres with extensive training and experience, particularly where further clarification of MR is needed.

Biventricular size and function assessment

The accurate assessment of ventricular volumes is crucial in the study of MVP. An increase in LV size or a reduction in LV ejection fraction are associated with a worse prognosis and are considered as an indication for surgery in patients with primary MR.³⁰ A thorough measurement of ventricular volumes is also required to reliably calculate the mitral RVol as the difference between LV–SV and aortic forward flow (or LVSV–RVSV in the absence of other valvular disease). The analysis of LV volumes by CMRI is based on the Simpson's method of disks. A stack of SSFP SA cine images is acquired from the base of the LV to the apex. The mitral valve annulus is conventionally considered the landmark that separates the LV from the LA; however, this approach has been proven to be inaccurate in patients with significant MVP and a three-long-axis method, which considers the mitral leaflets as the base of the LV, has been proposed to correct for this volume.³¹ In fact, the prolapsing leaflet in systole creates a space behind the mitral annulus, which is considered part of the LA although it contains the LV blood pool (Electronic [Supplementary Material Fig. S4](#)). The

conventional strategies, which ignore this part of the LV blood pool between the mitral annulus and the prolapsed leaflets, underestimate LVESV and consequently overestimate LVEF. A previous study has demonstrated that this “dead pool” could contribute along with the transvalvular MR to LV overload and remodelling.³² This concept could explain the LV dilatation disproportionate to the degree of MR, which has been described in patients with MVP, hence questioning the presence of a Barlow disease cardiomyopathy.^{33,34}

Assessment of left atrial size

In the clinical setting, LA diameters, areas, and volume are usually measured from SSFP cine images in different views and the values are indexed for body surface area (BSA). The LA appendage should be included as part of the

Table 5
Classification of mitral regurgitation severity by cardiac magnetic resonance imaging.

	Mild	Moderate	Severe	Very severe
Primary MR	RF <20%	RF 20–39%	RF 40–50% RVol >55–60 ml	RF >50%
Secondary MR	RVol <30 ml	RVol 30–60ml	RVol >60 ml	

Adapted from Garg P, Swift AJ, Zhong L et al. Assessment of mitral valve regurgitation by cardiovascular magnetic resonance imaging. *Nat Rev Cardiol.* 2020; 17:298–312.

MR, mitral regurgitation; RVol, regurgitant volume; RF, regurgitant fraction.

LA size while the pulmonary veins excluded; however, in daily practice both structures are excluded. Measurements are taken at maximal LA dimension, which is achieved during ventricular systole, defined as the last image before opening of the mitral valve on cine images. LA longitudinal and transverse diameters and area must be measured on 2C, 3C, and 4C cine bSSFP images (as illustrated in Electronic Supplementary Material Fig. S5), while LA volume can be measured by the modified Simpson’s method or the biplane area–length method. Corresponding reference values have been reported in the 2020 update for reference ranges for CMRI in adults and children.³⁵

Secondary findings

Once MVP is diagnosed, other associated cardiac defects should be spotted as prolapsing MV seems to be relatively common in a wide variety of congenital heart diseases. Specifically, MVP has been reported to be associated with secundum atrial septal defects and a consistent number of cases of association with Ebstein’s abnormality has been described in literature as well.³⁶ In addition, MVP may be found in the context of connective tissue disorders (such as Marfan syndrome, Loeys–Dietz syndrome, Ehlers–Danlos syndrome), aortic dilatation should always be excluded once a diagnosis of MVP is made. Should any of the above

abnormalities be suspected, a dedicated study is recommended to assess their severity and haemodynamic effects (Table 6).³⁷

LGE patterns

Several studies have described the presence of LGE in MVP patients.^{10,21,38–41} Due to the potential association between MVP and ventricular arrhythmias/SCD, it is always recommended to complete the CMRI study with contrast-enhanced imaging.^{11,12,42} Ten minutes after the administration of 0.1–0.2 mmol/kg gadolinium contrast agent, LGE sequences, i.e., inversion recovery (IR) or phase-sensitive inversion recovery (PSIR), should be acquired in the 2C, 3C, 4C and SA. Variable patterns of LGE (mid-wall, patchy, or subendocardial) have been documented, mainly in the inferior/inferolateral wall and/or the PMs (Electronic Supplementary Material Fig. S6).⁴³ Kitkungvan et al.⁴⁴ found the mid-wall striae as the most common pattern (12.6%), followed by patchy (8.1%) and subendocardial patterns (0.8%). The prevalence of replacement fibrosis among patients with MVP was more pronounced in the basal or mid inferolateral wall or basal inferior wall, which are the segments adjacent to the posteromedial PM. Perivalvular ventricular fibrosis and PMs fibrosis have been also described in pathology studies, and several reports have attributed PM scarring to abnormal tension with subsequent ischaemia.^{45,46} The substrate of electric instability in MVP may be the scarring of the PMs and of the LV inferolateral wall, in keeping with the anatomical origin of ventricular arrhythmias.²¹ An autopsy series has confirmed these findings, suggesting that LGE may enhance risk stratification of MVP patients considered as high-risk by clinical markers and especially complex ventricular arrhythmias.⁴¹ Interestingly, in the study of Pradella et al.⁴⁰ LGE was identified in about half of the MVP patients, independently of the degree of valve dysfunction and it was equally present in patients with or without arrhythmias. A recent review of the literature highlighted the controversial association of MVP with ventricular arrhythmias and SCD, emphasising the need for more evidence on its prognostic significance.³⁹

Table 6
Imaging protocols for associated abnormalities.

Scanning of secundum atrial septal defect	Scanning of dilated aorta	Scanning of Ebstein’s abnormality
<ul style="list-style-type: none"> • 4C cine view to measure RV size and identify the ASD • Ventricular SA cine stack for volume analysis • Atrial SA cine stack to identify the ASD • Modified 4C view through the ASD to visualise anterior and posterior septal rims • Oblique coronal view to visualise superior and inferior rims. • Modified oblique coronal view including IVC • En-face views of the ASD in the modified 4C and oblique coronal views • Through-plane flow above the PV and AV to quantify Qp/Qs • Flow through the ASD on en-face view 	<ul style="list-style-type: none"> • Transverse image stack through thorax to guide to the aortic anatomy • Oblique sagittal image stack through the longitudinal plane of the aorta. • The “candy-stick” cine view to display the thoracic aorta in a single slice • Transaxial aortic images to measure aortic diameters • Oblique coronal images of the descending aorta • LVOT view and LVOT cross-cut cine views for assessment of the sinuses and proximal ascending aorta • 3D-SSFP and contrast-enhanced MR angiography to visualise complex anatomy and detect dilation/stenosis 	<ul style="list-style-type: none"> • Transaxial cine stacks for volume analysis and assessment of TV coaptation • 4C, 2C, and RVLA cine views to visualise the TV leaflets • RVOT cine views to assess anatomy • Through-plane flow just above the PV for pulmonary flow • Through-plane flow just above the TV for TR quantification

4C, four-chamber; 2C, two-chamber; RV, right ventricle; ASD, atrial septal defect; IVC, inferior vena cava; PV, pulmonary valve; AV, aortic valve; Qp, pulmonary flow, Qs, systemic flow; 3C, three-chamber; LVOT, left ventricular outflow tract; SSFP, steady state free precession; MR, magnetic resonance; TV, tricuspid valve; RVLA, right ventricular long axis; RVOT, right ventricle outflow tract; TR, tricuspid regurgitation.

Myocardial T1 mapping

The qualitative analysis of unenhanced and contrast-enhanced T1 maps is helpful to confirm the areas of fibrosis showed by LGE. Patients with MVP have higher native T1 values and increased ECV compared to controls even in the absence of LGE.⁴⁰ Diffuse fibrosis of the LV septum and higher ECV values may be found in MVP patients although their prognostic significance remains unknown.⁴²

Summary

In conclusion, further to the assessment of MVP by echocardiography, a comprehensive CMRI study of MVP may provide additional findings regardless of the severity of valve dysfunction. CMRI allows comprehensive evaluation of the

prolapsing valve and its haemodynamic impact on cardiac chambers, as well as the presence of mitral annulus disjunction, focal LV hypertrophy, and myocardial fibrosis, which are well-established markers of arrhythmic/SCD risk in MVP.

Conflict of interest

The authors declare that they have no known competing financial interests or personal relationships that could have appeared to influence the work reported in this paper.

Acknowledgements

L.L.M. was supported by a research grant provided by the Cardiopath PhD programme. The funder had no involvement in the study design, in the collection and interpretation of data.

Appendix A. Supplementary data

Supplementary data to this article can be found online at <https://doi.org/10.1016/j.crad.2021.11.004>.

References

- Delling FN, Vasan RS. Epidemiology and pathophysiology of mitral valve prolapse: new insights into disease progression, genetics, and molecular basis. *Circulation* 2014;**129**(21):2158–70.
- Dormand H, Mohiaddin RH. Cardiovascular magnetic resonance in Marfan syndrome. *J Cardiovasc Magn Reson* 2013;**15**:33.
- Le Tourneau T, Merot J, Rimbert A, et al. Genetics of syndromic and non-syndromic mitral valve prolapse. *Heart* 2018;**104**(12):978–84.
- Prunier F, Terrien G, Le Corre Y, et al. Pseudoxanthoma elasticum: cardiac findings in patients and Abcc6-deficient mouse model. *PLoS One* 2013;**8**(7):e68700.
- Han Y, Peters DC, Salton CJ, et al. Cardiovascular magnetic resonance characterization of mitral valve prolapse. *JACC Cardiovasc Imaging* 2008;**1**(3):294–303.
- Ricci F, Aung N, Gallina S, et al. Cardiovascular magnetic resonance reference values of mitral and tricuspid annular dimensions: the UK Biobank cohort. *J Cardiovasc Magn Reson* 2020;**23**(1):5.
- Avierinos JF, Gersh BJ, Melton 3rd LJ, et al. Natural history of asymptomatic mitral valve prolapse in the community. *Circulation* 2002;**106**(11):1355–61.
- Essayagh B, Sabbag A, Antoine C, et al. Presentation and outcome of arrhythmic mitral valve prolapse. *J Am Coll Cardiol* 2020;**76**(6):637–49.
- Gati S, Malhotra A, Sharma S. Exercise recommendations in patients with valvular heart disease. *Heart* 2019;**105**(2):106–10.
- Perazzolo Marra M, Basso C, De Lazzari M, et al. Morphofunctional abnormalities of mitral annulus and arrhythmic mitral valve prolapse. *Circ Cardiovasc Imaging* 2016;**9**(8):e005030.
- Carmo P, Andrade MJ, Aguiar C, et al. Mitral annular disjunction in myxomatous mitral valve disease: a relevant abnormality recognizable by transthoracic echocardiography. *Cardiovasc Ultrasound* 2010;**8**:53.
- Eriksson MJ, Bitkover CY, Omran AS, et al. Mitral annular disjunction in advanced myxomatous mitral valve disease: echocardiographic detection and surgical correction. *J Am Soc Echocardiogr* 2005;**18**(10):1014–22.
- Newcomb AE, David TE, Lad VS, et al. Mitral valve repair for advanced myxomatous degeneration with posterior displacement of the mitral annulus. *J Thorac Cardiovasc Surg* 2008;**136**(6):1503–9.
- Lee AP, Jin CN, Fan Y, et al. Functional implication of mitral annular disjunction in mitral valve prolapse: a quantitative dynamic 3D echocardiographic study. *JACC Cardiovasc Imaging* 2017;**10**(12):1424–33.
- Bennett S, Thamman R, Griffiths T, et al. Mitral annular disjunction: a systematic review of the literature. *Echocardiography* 2019;**36**(8):1549–58.
- Essayagh B, Sabbag A, Antoine C, et al. The mitral annular disjunction of mitral valve prolapse: presentation and outcome. *JACC Cardiovasc Imaging* 2021 Nov;**14**(11):2073–87. <https://doi.org/10.1016/j.jcmg.2021.04.029>.
- Dejgaard LA, Skjoldvik ET, Lie OH, et al. The mitral annulus disjunction arrhythmic syndrome. *J Am Coll Cardiol* 2018;**72**(14):1600–9.
- Basso C, Iliceto S, Thiene G, et al. Mitral valve prolapse, ventricular arrhythmias, and sudden death. *Circulation* 2019;**140**(11):952–64.
- Fulton BL, Liang JJ, Enriquez A, et al. Imaging characteristics of papillary muscle site of origin of ventricular arrhythmias in patients with mitral valve prolapse. *J Cardiovasc Electrophysiol* 2018;**29**(1):146–53.
- Mantegazza V, Volpato V, Gripari P, et al. Multimodality imaging assessment of mitral annular disjunction in mitral valve prolapse. *Heart* 2021;**107**(1):25–32.
- Basso C, Perazzolo Marra M, Rizzo S, et al. Arrhythmic mitral valve prolapse and sudden cardiac death. *Circulation* 2015;**132**(7):556–66.
- Essayagh B, Iacuzio L, Civaia F, et al. Usefulness of 3-tesla cardiac magnetic resonance to detect mitral annular disjunction in patients with mitral valve prolapse. *Am J Cardiol* 2019;**124**(11):1725–30.
- Zia MI, Valenti V, Cherston C, et al. Relation of mitral valve prolapse to basal left ventricular hypertrophy as determined by cardiac magnetic resonance imaging. *Am J Cardiol* 2012;**109**(9):1321–5.
- Penicka M, Vecera J, Mirica DC, et al. Prognostic implications of magnetic resonance-derived quantification in asymptomatic patients with organic mitral regurgitation: comparison with Doppler echocardiography-derived integrative approach. *Circulation* 2018;**137**(13):1349–60.
- Devos DGH, Kilner PJ. Calculations of cardiovascular shunts and regurgitation using magnetic resonance ventricular volume and aortic and pulmonary flow measurements. *Eur Radiol* 2010;**20**:410–21.
- Chan KM, Wage R, Symmonds K, et al. Towards comprehensive assessment of mitral regurgitation using cardiovascular magnetic resonance. *J Cardiovasc Magn Reson* 2008;**10**:61.
- Garg P, Swift AJ, Zhong L, et al. Assessment of mitral valve regurgitation by cardiovascular magnetic resonance imaging. *Nat Rev Cardiol* 2020;**17**:298–312.
- Fidock B, Archer G, Barker N, et al. Standard and emerging CMRI methods for mitral regurgitation quantification. *Int J Cardiol* 2021;**331**:316–21.
- Fidock B, Barker N, Balasubramanian N, et al. A systematic review of 4D-flow MRI derived mitral regurgitation quantification methods. *Front Cardiovasc Med* 2019;**6**:103.
- Baumgartner H, Falk V, Bax JJ, et al. ESC/EACTS guidelines for the management of valvular heart disease. *Eur Heart J* 2017;**38**(36):2739–91. 2017.
- Vincenti G, Masci PG, Rutz T, et al. Impact of bileaflet mitral valve prolapse on quantification of mitral regurgitation with cardiac magnetic resonance: a single-center study. *J Cardiovasc Magn Reson* 2017;**19**(1):56.
- Bach DS. Dead pool: a non-regurgitant volume overload among patients with barlow mitral valve prolapse. *JACC Cardiovasc Imaging* 2021;**14**(3):585–7.
- Yiginer O, Keser N, Ozmen N, et al. Classic mitral valve prolapse causes enlargement in left ventricle even in the absence of significant mitral regurgitation. *Echocardiography* 2012;**29**(2):123–9.
- El-Tallawi KC, Kitkungvan D, Xu J, et al. Resolving the disproportionate left ventricular enlargement in mitral valve prolapse due to barlow disease: insights from cardiovascular magnetic resonance. *JACC Cardiovasc Imaging* 2021;**14**(3):573–84.
- Kawel-Boehm N, Hetzel SJ, Ambale-Venkatesh B, et al. Reference ranges ("normal values") for cardiovascular magnetic resonance (CMR) in adults and children: 2020 update. *J Cardiovasc Magn Reson* 2020;**22**(1):87.
- Cabin HS, Roberts WC. Ebstein's anomaly of the tricuspid valve and prolapse of the mitral valve. *Am Heart J* 1981;**101**(2):177–80.
- Myerson SG, Francis J, Neubauer S. *Cardiovascular magnetic resonance (oxford specialist handbooks in cardiology)*. Oxford: Oxford University Press; 2010.
- Perazzolo Marra M, De Lazzari M, Zorzi A, et al. Impact of the presence and amount of myocardial fibrosis by cardiac magnetic resonance on arrhythmic outcome and sudden cardiac death in nonischemic dilated cardiomyopathy. *Heart Rhythm* 2014;**11**(5):856–63.
- Spartalis M, Tzatzaki E, Spartalis E, et al. Mitral valve prolapse: an underestimated cause of sudden cardiac death—a current review of the literature. *J Thorac Dis* 2017;**9**(12):5390–8.

40. Pradella S, Grazzini G, Brandani M, et al. Cardiac magnetic resonance in patients with mitral valve prolapse: focus on late gadolinium enhancement and T1 mapping. *Eur Radiol* 2019;**29**(3):1546–54.
41. Sheppard MN, Steriotis AK, Sharma S. Letter by Sheppard et al regarding article, "Arrhythmic mitral valve prolapse and sudden cardiac death. *Circulation* 2016;**133**(13):e458.
42. Bui AH, Roujol S, Foppa M, et al. Diffuse myocardial fibrosis in patients with mitral valve prolapse and ventricular arrhythmia. *Heart* 2017;**103**(3):204–9.
43. Han HC, Ha FJ, Teh AW, et al. Mitral valve prolapse and sudden cardiac death: a systematic review. *J Am Heart Assoc* 2018;**7**(23):e010584.
44. Kitkungvan D, Nabi F, Kim RJ, et al. Myocardial fibrosis in patients with primary mitral regurgitation with and without prolapse. *J Am Coll Cardiol* 2018;**72**(8):823–34.
45. Dollar AL, Roberts WC. Morphologic comparison of patients with mitral valve prolapse who died suddenly with patients who died from severe valvular dysfunction or other conditions. *J Am Coll Cardiol* 1991;**17**(4):921–31.
46. Farb A, Tang AL, Atkinson JB, et al. Comparison of cardiac findings in patients with mitral valve prolapse who die suddenly to those who have congestive heart failure from mitral regurgitation and to those with fatal noncardiac conditions. *Am J Cardiol* 1992;**70**(2):234–9.